

Contrasting whole-tree water use, hydraulics, and growth in a co-dominant diffuse-porous vs. ring-porous species pair

Erica I. von Allmen · John S. Sperry ·
Susan E. Bush

Received: 28 April 2014 / Revised: 10 November 2014 / Accepted: 16 December 2014 / Published online: 24 December 2014
© Springer-Verlag Berlin Heidelberg 2014

Abstract

Key message Greater transport capacity of diffuse- vs. ring-porous stem networks translated into greater water use by the diffuse-porous co-dominant, but similar growth indicated higher water use efficiency of the ring-porous species.

Abstract Coexistence of diffuse- vs. ring-porous trees in north-temperate deciduous forests implies a complementary ecology. The contrasting stem anatomies may result in divergent patterns of water use, and consequences for growth rate are unknown. We investigated tree hydraulics and growth rates in two co-dominants: diffuse-porous *Acer grandidentatum* (“maple”) and ring-porous *Quercus gambelii* (“oak”). Our goals were (1) document any differences in seasonal water use and its basis in divergent stem anatomy and (2) compare annual growth rates and hence growth-based water use efficiencies. At maximum transpiration, maple trees used more than double the water than oak trees. Maple also had more leaf area per basal area, resulting in similar water use per leaf area between species. Maple had ca. double the tree hydraulic conductance than oak owing to greater conductance of its diffuse-porous stem network (leaf- and root system conductances were less different between species). Water use in maple increased with vapor pressure deficit (VPD), whereas in

oak it decreased very slightly indicating a more sensitive stomatal response. Seasonably stable water use and xylem pressure in oak suggested a deeper water source. Although maple used more water, both species exhibited similar annual biomass growth of the above-ground shoot network, indicating greater growth-based water use efficiency of oak shoots. In sum, water use in maple exceeded that in oak and was more influenced by soil and atmospheric water status. The low and stable water use of oak was associated with a greater efficiency in exchanging water for shoot growth.

Keywords Water use efficiency · Ecological wood anatomy · Xylem structure and function · Hydraulic architecture · Metabolic scaling · Tree ecophysiology

Introduction

Coexistence of ring- and diffuse-porous species is the rule for many north-temperate deciduous forests (Barbour and Billings 1988), suggesting the two tree types maintain a competitive balance despite their contrasting stem wood anatomy. Diffuse-porous trees rely on multiple growth rings of relatively narrow vessels for stem water transport, whereas ring-porous trees transport water through typically one ring of large earlywood stem vessels (the latewood vessels are too few and narrow to carry much transpirational flow; Zimmermann 1983). The difference in anatomy has implications for the duration and quantity of water transport during the growing season. But less is known of whether contrasts in stem anatomy and water transport translate into differences in growth rate, a trait critical for competitive ability. Our goal was first to document seasonal water use and associated hydraulic traits in a co-dominant species pair with diffuse vs. ring-porous stem

Communicated by M. Zwieniecki.

E. I. von Allmen
Department of Botany, University of Hawaii, 96822 Honolulu,
HI, USA

J. S. Sperry (✉) · S. E. Bush
Department of Biology, University of Utah,
84112 Salt Lake City, UT, USA
e-mail: j.sperry@utah.edu

anatomies, and second to compare the efficiency of the exchange between water use and growth of the above-ground shoot (stem network + leaves) between the two species.

Trade-offs between diffuse- vs. ring-porous architectures probably underlie their coexistence in temperate hardwood forests. The two anatomical types have distinct differences concerning the problem of winter xylem embolism. The narrower vessels of diffuse-porous trees (e.g., $<50\ \mu\text{m}$) are less vulnerable to embolism by freeze–thaw cycles, and many species have mechanisms for generating positive xylem pressures in early spring to refill any vessels that have embolized (Hacke and Sauter 1996; Davis et al. 1999). The genus *Acer*, for example, can refill by stem pressures in early spring, as well as by root pressure (Sperry et al. 1988). Resistance to freeze–thaw embolism and spring refilling enables multiple growth rings to be active for growing season transport. Bud-burst occurs relatively early in spring, consistent with minimal vascular vulnerability to the occasional spring freeze. In contrast, the much wider vessels of ring-porous trees (e.g., $>100\ \mu\text{m}$) are exceedingly vulnerable to freeze–thaw embolism, but are also much more efficient (per vessel) at water transport. Hence, rather than refilling previous year's vessels, ring-porous trees produce a new set of relatively few, but efficient, vessels in concert with bud-burst (Zimmermann 1983). However, bud-burst occurs considerably later in spring when the risk of an embolism-inducing freeze is very low (Wang et al. 1992; Jaquish and Ewers 2001). The ring- vs. diffuse-porous distinction applies to stem xylem, and not coincidentally, because stems are the part of the tree most exposed to freezing temperatures. Root wood of ring-porous trees can maintain multiple years of functional sapwood (Jaquish and Ewers 2001), and where examined their anatomy is not qualitatively different from the typically wide-vesseled root wood of diffuse-porous trees (Gasson 1985).

There are also different responses of diffuse- vs. ring-porous species to growing season water stress. The narrow vessels in diffuse-porous stems are associated with a wide range in vulnerability, with some species being very resistant to embolism (Hacke et al. 2006). In contrast, the larger vessels of ring-porous stems may make this tree type more uniformly vulnerable to embolism by water stress (Bush et al. 2008; Litvak et al. 2012). Although the diffuse- vs. ring-porous comparison is complicated by possible artifacts in determining vulnerability to embolism in large-vesseled species (Cochard et al. 2010), recent studies on ring-porous *Q. gambelii* support high vulnerability of a sizeable fraction of the large vessels (Christman et al. 2012; Sperry et al. 2012a). *Q. gambelii* stems are reported to lose 50 % of its hydraulic conductivity at a xylem pressure of about -1.1 vs. -3.5 MPa in co-occurring

diffuse-porous *Acer grandidentatum* (Alder et al. 1996; Christman et al. 2012).

If there is indeed a general distinction between vulnerability to cavitation by water stress in these two functional groups, the more vulnerable ring-porous species might be expected to protect their stem xylem from exposure to low pressures by some combination of deep rooting, isohydric stomatal regulation of canopy xylem pressure (i.e., a strong response to vapor pressure deficit, VPD), and habitat (Bush et al. 2008). The differences in wood anatomy and vulnerability could also translate into differences in absolute rates of water consumption, whole-tree hydraulic conductance, and growth rates. Is the same amount of water transported in the relatively few large current year vessels of a ring-porous stem network as in the exceedingly more numerous but narrow vessels of a diffuse-porous one? And is water usage per growth comparable between the two tree types?

In this paper, we conduct a comprehensive comparison of water use, whole-tree hydraulic conductance, and growth rates over a season between co-occurring *A. grandidentatum* (diffuse-porous) and *Q. gambelii* (ring-porous). These two species form a shrub-woodland in the Intermountain West of the U.S. between the low elevation grass-shrublands and the high elevation spruce-fir forests (Barbour and Billings 1988). Typical of the region, the oak-maple woodland receives the majority of its annual precipitation as winter snow and experiences a predictable summer drought. Like the extensively studied *Pinyon-Juniper* woodlands of the Colorado Plateau and southwards, the simple *Acer-Quercus* community provides an opportunity for understanding how co-dominant species partition limited water resources.

Our *Acer-Quercus* comparison was designed to detect inherent differences between the species, so trees were studied along a riparian corridor to minimize variation in soil water supply, and results were normalized for variation in tree size. Our goals were (1) to document and explain inherent differences in water use, particularly their linkage to divergent stem anatomy, and (2) determine whether differences in water use efficiency modulate how water usage corresponds to net growth of the above-ground branching system. Water use and hydraulic conductances were expressed on both a whole-tree and leaf-area basis. We partitioned tree conductance into root, stem, and leaf components, expecting any differences to be mainly confined to stems where the ring- vs. diffuse-porous differences are manifest. Although a portion of the results have been published in a study designed to test a theoretical model of metabolic scaling (von Allmen et al. 2012), here we report additional data and analyses of the comparative ecophysiology of the *Acer-Quercus* species pair.

Materials and methods

Study sites

We studied three natural stands of *A. grandidentatum* (Nutt) (“maple” hereafter) and *Q. gambelii* (Nutt) (“oak”) in the riparian zone of Red Butte Canyon Research Natural Area approximately 8 km east of Salt Lake City, Utah (40°47’N and 111°48’W, stands at 1,660, 1,680, 1,730 m elevation). The area receives roughly 500 mm of annual precipitation mostly as snow in the winter (Ehleringer et al. 1992). Stands were selected to have continuous canopy without isolated individuals.

Climate and meteorological data

Temperature and percent relative humidity were measured (HMP35C, HMP50, CS500; Campbell Scientific, Logan, Utah) at each stand every 30 s and averaged and stored every 30 min in dataloggers (CR7X; Campbell Scientific, Logan, Utah) from June through September 2009. The air temperature and relative humidity were used to calculate atmospheric vapor pressure deficit (VPD). Photosynthetic active radiation (PAR) was measured with a Li-cor quantum sensor (LI-190SZ, Li-cor Biosciences, Lincoln, Nebraska) every 30 s and averaged every 30 min by a datalogger (CR10X; Campbell Scientific, Logan, Utah) roughly 1 km away at an existing weather station in Red Butte Canyon. Daily precipitation was measured at the same weather station with a tipping-bucket rain gauge (TE525; Campbell Scientific, Logan, Utah).

Whole-tree sapflow

Whole-tree sapflow (*Q*, Table 1 lists important symbols used) was measured across a range of tree diameters (*D*) in each species from Red Butte Canyon RNA (oak *D*: 4–23 cm, maple *D*: 5–26 cm). The upper diameter range approached the maximum for this riparian forest. At each of the three sites, 6 trees per species were selected with upper canopies in full sun. Across sites there was a total 18 individuals from each species. Trees were rooted 17–34 m away from the stream, and 6–9 m above the stream surface.

The rate of water transport was measured at each tree using heat dissipation sensors (Granier 1985). Granier sensors measure the temperature difference (ΔT) between a constantly heated downstream sensor and an unheated sensor located upstream. Paired sensors were inserted 15 cm apart (axially) on random sides of the tree trunk at breast height. Standard Granier probes (20 mm long) were used in maple, while shorter probes (10 mm long) were used for oak because of its shallow active xylem layer. Sap flowing past the heated sensor dissipates heat and minimizes ΔT . The ΔT relative to the maximum value at zero flow (ΔT_m) is empirically related to the sap flow per sapwood area $J_s = a((\Delta T_m/\Delta T) - 1)^b$. Parameters *a* and *b* are best-fit values. The ΔT was measured every 30 s and averaged every 30 min using dataloggers (CR7X, Campbell Scientific, Logan, Utah) from mid-June until leaf senescence (June 15–Oct 31, 2009). Tree *Q* was expressed as daily sums, mid-day averages, and mid-day maximum per tree (Q_{max} , see below).

Table 1 Frequently used symbols, their definitions, and units employed

Symbol, definition	Units
A_L , leaf area	cm ²
A_B , basal area of twig or trunk	cm ²
<i>D</i> , trunk diameter above root collar	cm
<i>K</i> , tree hydraulic conductance	kg hr ⁻¹ MPa ⁻¹
K_s , size-standardized tree hydraulic conductance	kg hr ⁻¹ MPa ⁻¹ cm ^{-q}
P_{PD} , predawn xylem pressure	MPa
P_{MD} , P_{RC} mid-day leaf pressure, root crown pressure	MPa
ΔP , total soil-canopy mid-day pressure drop	MPa
$\Delta P'$, mid-day pressure drop minus gravitational component	MPa
<i>Q</i> , tree sapflow rate	kg hr ⁻¹
Q_{max} , seasonal maximum mid-day sapflow rate	kg hr ⁻¹
Q_L , seasonal maximum mid-day sapflow per leaf area	kg hr ⁻¹ m ⁻²
Q_s , size-standardized mid-day sapflow rate	kg hr ⁻¹ cm ^{-q}
<i>q</i> , Q_{max} by D^q scaling exponent	–
R_{tree} , tree hydraulic resistance = 1/ <i>K</i>	hr MPa kg ⁻¹
R_{shoot} , R_{root} , hydraulic resistance in shoot and root system	hr MPa kg ⁻¹
R_{leaf} , R_{stem} , hydraulic resistance in leaves and stem network	hr MPa kg ⁻¹
r_{leaf} , area-specific resistance of individual leaf	s kPa m ² mg ⁻¹

Recent tests have validated Granier's original calibration, where $a = 0.119 \text{ mm s}^{-1}$ and $b = 1.23$ for diffuse-porous species (20 mm probes) growing in the Salt Lake City area, but indicate that new calibrations are necessary for ring-porous species (Bush et al. 2010). Therefore, we used Granier's coefficients for maple, but calibrated oak as described in von Allmen et al. (2012). The oak calibration gave $a = 7.17 \text{ mm s}^{-1}$ and $b = 1.33$ (von Allmen et al. 2012).

To obtain whole-tree sapflow ($Q = J_s \times A_{sw}$) from sensors in the field, total cross-sectional sapwood area (defined as active conducting area, A_{sw}) was calculated from sapwood depth measured from tree cores. A single core was collected from each experimental tree using a 12-mm increment borer (Haglöf, Sweden). In the oak, water transport was only detectable in the outermost ring of earlywood vessels, as indicated by dye perfusions used to calibrate the oak sensors (von Allmen et al. 2012). Conducting sapwood area in oak was estimated by measuring the area of the current year's ring of large earlywood vessels (equivalent to the area of the narrow dye-stained ring in the calibrated stems). To determine actively conducting sapwood area in maple, holes were drilled under water into the center of the trunk and injected with 0.1 % Safranin O dye. This was performed at mid-day only on full sun days. Cores were taken from the height between the sensors (10 cm above the dye injection site) after trees had transpired dye for 1 h. The dyed sapwood depth was used to calculate the conducting sapwood area (A_{sw}). A correction according to Clearwater (1999) was applied in cases where maple probe length exceeded the depth of sapwood.

We also expressed tree water use per canopy leaf area (Q_L). Canopy leaf area was approximated from the average leaf area per basal area (A_L/A_B) for each species. The A_L/A_B was measured on current year leaf-bearing twigs ($n = 22$ maple, $n = 64$ oak; collected from multiple trees). The ratio did not vary significantly with twig basal area, and it was assumed not to vary with trunk basal area. Previous work indicated that the study trees exhibited approximate area-preserving branching (Da Vinci's rule; von Allmen et al. 2012), so the trunk basal area is approximated by the collective cross-sectional area of all twigs. Under these conditions, the average A_L/A_B at the twig level provides a rough estimate of the A_L/A_B of the tree. Canopy leaf area was obtained by multiplying A_L/A_B by the trunk basal area for each study tree. Tree Q was divided by its total canopy leaf area to give Q_L .

To estimate the effects of tree size on water use we filtered the dataset to obtain daily maximum sapflow per tree (Q_{max}) under well-watered, full sun, and high VPD conditions. Maximum sapflow will be limited only by

stomatal regulation of canopy xylem pressure rather than by low light, soil moisture, or VPD. Thus, to obtain Q_{max} we avoided data from cloudy days or from late summer periods for maple where its predawn xylem pressures became more negative than -1 MPa , indicating soil drought in the rooting zone. In addition, we selected days whose mean VPD (daily means of 30 min means) was within the 90th percentile for the season. The Q_{max} for each tree was the average of the top five 30 min Q means for each selected day, averaged again over all selected days from the 100 day "peak growing season" from late June to early September (Fig. 3a, vertical dotted lines). The relationship of tree Q_{max} and diameter (D) gave the scaling exponent q ($Q_{max} \propto D^q$). The confounding effect of tree size in subsequent comparisons was removed by dividing sapflow by D^q ($Q_s = Q/D^q$), where Q_s refers to the size-standardized water flow rate. As long as " q " is similar between species (as proved to be the case), this removes the size effect both within and across species.

To assess the response of water use to vapor pressure deficit, we plotted mid-day Q_s (average of top five 30 min means) vs. mid-day VPD (average of 30 min means for same 5 intervals) over the full VPD range during the peak growing season. As with tree Q_{max} , we avoided data from cloudy days or from periods where predawn xylem pressures in maple fell below -1 MPa .

Whole-tree hydraulic conductance (K)

Xylem pressures were measured at roughly 10 day intervals over the growing season on the sapflow trees. Pressures were measured on excised leaves ($n = 3$ per tree) with a Scholander pressure chamber (PMS Instruments Co., Corvallis, Oregon). On a given date, up to three types of pressure measurements were made for each tree: predawn pressures from leaves near ground level (P_{PD} ; 0400–0600 h, assumed to approximate soil water potential in the rooting zone), mid-day canopy pressure (P_{MD} ; 1100–1400 h), and mid-day root-crown pressure (P_{RC} ; 1200–1400 h). To measure P_{RC} , we covered all leaves on shoots attached near the root crown with foil and allowed xylem pressures to equilibrate with the root crown pressure for 1 h at mid-day on full sun days. Covered leaves were then cut and immediately measured in the pressure chamber. Because of limitations on the number of shoots available for P_{RC} measurements, we could only measure P_{RC} on a subset of measurement days.

Soil to canopy pressure drop (ΔP) was calculated from $P_{PD} - P_{MD}$. To account for tree height, we subtracted the drop in pressure due to gravity ($\Delta P'$; $\Delta P' = \Delta P - \rho g H$, where P is in MPa, and H is tree height in meters, and $\rho g = 0.009781$ in MPa/m). The $\Delta P'$ is the pressure drop associated with the transpiration stream. Given the

relatively short heights of our trees (<12 m) the gravitational effect was small, and $\Delta P'$ was independent of tree size within each species (von Allmen et al. 2012). The estimated whole-tree conductance (K_s) for each tree was the mid-day size-standardized Q_s divided by $\Delta P'$ ($K_s = Q_s/\Delta P'$). Thus, K_s values were also effectively corrected for size-dependence. Standardized whole-tree conductances were averaged over all individuals at each site at each sampling date. For days when P_{PD} , P_{RC} , and P_{MD} were measured on the same trees, we estimated $\Delta P_{shoot}/\Delta P$ from $(P_{RC} - P_{MD})/(P_{PD} - P_{MD})$. The $\Delta P_{shoot}/\Delta P$ ratio equates to the fraction of whole-tree hydraulic resistance in the shoot system.

Estimating root, stem, and leaf hydraulic resistances

To partition tree hydraulic conductance into root, stem, and leaf components we converted to resistances ($R = 1/K$) which are additive in series. The $\Delta P_{shoot}/\Delta P$ ratio was size independent (von Allmen et al. 2012), so we were able to partition whole-tree resistance ($R_{tree} = 1/K$) into total root system resistance (R_{root}) and shoot system resistance (R_{shoot}). The tree K was obtained from $K_s \times D^q$, where K_s was the species average (K_s was seasonally stable, see “Results”). This allowed us to predict R_{shoot} and R_{root} as a continuous function of D .

We further partitioned the shoot hydraulic resistance R_{shoot} into series components of the stem network (R_{stem}) and the collective leaves (R_{leaf}). The leaf-area-specific leaf resistance of individual leaves (r_{leaf}) was measured on 12 leaves per species. For purposes of comparing species and testing effects of tree size we sampled sun leaves for consistency. One leaf was sampled from each of 12 trees with a range of trunk diameters ($D = 4\text{--}32$ cm) similar to the sap flux individuals. Sun leaves typically have lower r_{leaf} than shade leaves (Sack and Tyree 2005), so our sampling strategy yielded a deliberate low-end estimate of R_{leaf} . This bias should not influence relative values between species and tree sizes.

The r_{leaf} was measured with the evaporative flux method (Sack et al. 2002). A 1–2 cm twig apex bearing a mature terminal leaf was excised underwater and immediately fixed to tubing filled with 20-mM KCl in distilled water in direct sunlight. While the leaf transpired, the rate of solution uptake was recorded. When a stable rate had been obtained, the leaf was covered with foil and simultaneously cut with a sharp razor blade and bulk leaf xylem pressure measured in a pressure chamber. The r_{leaf} was calculated as the xylem pressure divided by the uptake rate, all multiplied by the area of the measured leaf (determined later with an area meter; LI-COR 3100, Lincoln, Nebraska, USA). The r_{leaf} was standardized to 20 °C to correct for variation in water viscosity with

measurement temperature. Although a short section of twig xylem was included in the measurement, r_{leaf} was assumed to be overwhelmingly determined by the leaf. After finding no relationship between r_{leaf} and tree size (D), the r_{leaf} was averaged for each species ($n = 12$ leaves). The oak mean excluded one outlier that was 2.9 standard deviations above the mean because of an exceptionally low transpiration rate. The average r_{leaf} was divided by the estimated leaf area of the tree (A_L , see above) to obtain an estimate of parallel resistance of all leaves ($R_{leaf} = r_{leaf}/A_L$). The resistance of the stem network (R_{stem}) was estimated by subtraction: $R_{stem} = R_{shoot} - R_{leaf}$.

Stem biomass growth estimates

Biomass growth of the above-ground branching network was estimated previously for the same study trees (von Allmen et al. 2012 for details). Here we report these data with the addition of the leaf biomass. Briefly, we estimated how the volume of the stem network scaled with D from height by diameter allometry relationships for both species at the study site. Volume scaling was converted to mass scaling from wood density measurements. The annual growth in D was reconstructed for each study tree from growth ring and bark thickness data taken from cores of each sap flux tree. Annual biomass growth (kg dry mass per year) of stems was estimated from the increase in mass associated with each annual increment in D . The leaf mass per D was estimated from the specific leaf area (leaf area per dry mass, $\text{cm}^2 \text{g}^{-1}$) and the leaf area per basal area (already described). In this way, the annual stem + leaf biomass growth was estimated over the life of each experimental tree, as well as for just the 2009 growing season for which we measured water consumption (von Allmen et al. 2012).

Statistics

Power functions were often used to describe relationships between variables. These were obtained by linear regression through log-transformed data. Following the advice of Warton et al. (2006), we used ordinary least squares (OLS) regression when the purpose was to predict a specific “y” value from a given “x” value. We used reduced major axis (RMA) regression when the purpose was to estimate the slope of the relationship (the scaling exponent). To analyze intra-specific differences in maple and oak regressions, homogeneity of regression slopes was performed in SPSS (SPSS, Inc. 1986, version 10). A standard t test was used to test slopes and compare means between species ($p = 0.05$ significance threshold).

Results

Effects of tree size, leaf area, and vapor pressure deficit on water use

During mid-summer periods that maximized transpiration, maple transported 1.7–2.6 times more water than oak across all tree diameters (Fig. 1, circles). The maximum tree sapflow (Q_{\max}) scaled with tree diameter (D^q) to an RMA regression exponent $q = 1.56$ in maple (95 % confidence limit 1.24–1.88) and $q = 1.58$ in oak (1.05–2.12). This size-function relationship with a scaling exponent of less than $q = 2$ means that larger trees used less water per basal area than smaller ones. The similarity between oak and maple scaling exponents allowed us to remove the confounding effect of tree size in cross species comparison by dividing Q by D^q ($Q_s = Q/D^q$).

When Q_{\max} was expressed per estimated canopy leaf area ($Q_L = Q_{\max}/A_L$), there was no difference between species (Fig. 1 squares). This was because the estimated leaf area per basal area (A_L/A_B) was greater in maple ($2,160 \pm 199 \text{ cm}^2 \cdot \text{cm}^{-2}$, mean \pm SE) than oak ($1,160 \pm 66 \text{ cm}^2 \cdot \text{cm}^{-2}$). The Q_L declined with tree size because A_L was assumed to increase in proportion with A_B whereas Q was found to increase more slowly with A_B (i.e., $q < 2$).

Maple mid-day mean sapflow (Q_s , standardized for tree size) increased with VPD (linear regression: $P < 0.01$, $r^2 = 0.26$; Fig. 2 shows the slightly better fit of a saturation to maximum curve, $r^2 = 0.27$), whereas oak sapflow actually declined slightly (linear regression: $P < 0.05$, $r^2 = 0.09$). The two species have similar leaf widths, and were growing together in the same stands, thus likely experiencing similar coupling to atmospheric VPD. For this reason, their

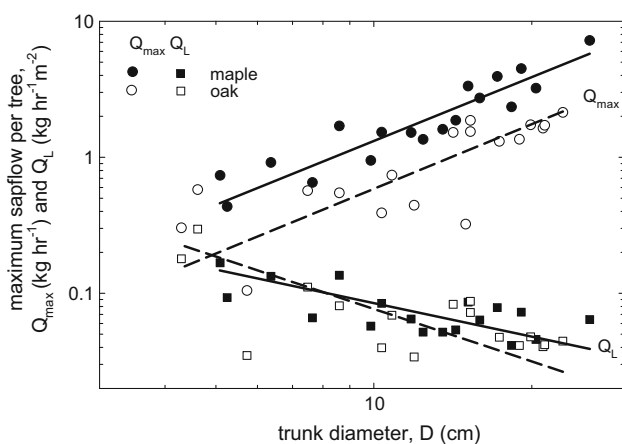


Fig. 1 Maximum sapflow per tree (Q_{\max} , circles) and per tree leaf area (Q_L , squares) for *Acer grandidentatum* (maple, solid symbols) and *Quercus gambelii* (oak, open square symbols) shown as a function of tree diameter (D). Linear RMA regressions (maple solid, oak dashed) shown. The Q_{\max} by D^q scaling exponent was $q = 1.56$ ($r^2 = 0.85$) for maple and $q = 1.58$ ($r^2 = 0.59$) for oak

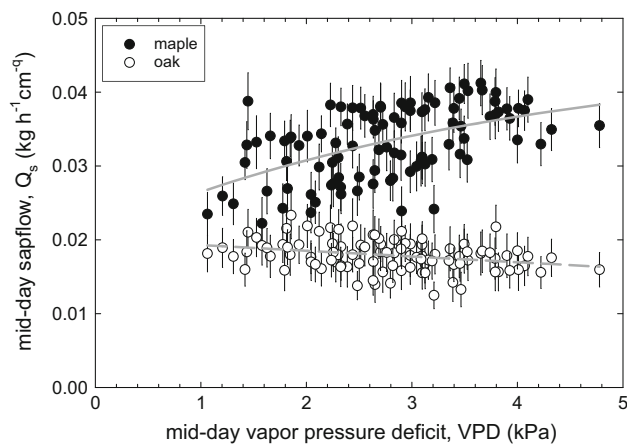


Fig. 2 Mid-day sapflow (Q_s , standardized for tree size) versus mid-day atmospheric vapor pressure deficit (VPD) for *Acer grandidentatum* (maple) and *Quercus gambelii* (oak). Maple data were fit with exponential saturation curve ($Q_s = a(1 - e^{-b \times \text{VPD}})$; $r^2 = 0.27$), though a linear regression gave nearly as good a fit ($r^2 = 0.26$); oak data were fit with a (statistically significant) linear regression ($r^2 = 0.09$)

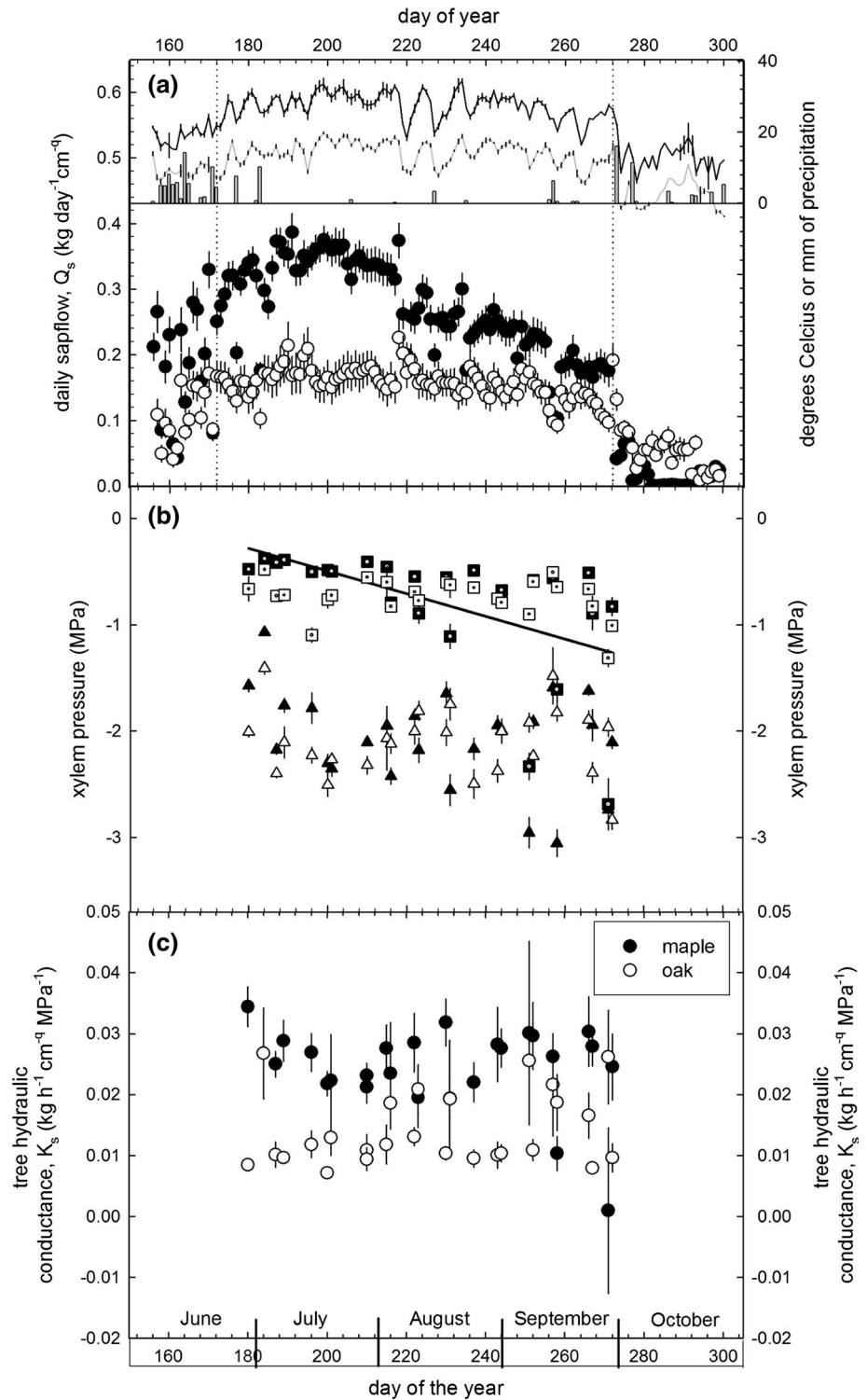
significantly divergent VPD behavior likely resulted from divergent stomatal sensitivity to VPD, with oak having the more sensitive response. The constancy of Q_s in oak would minimize any VPD-associated drop in xylem pressure.

Seasonal tree water use and hydraulic conductance

The average mid-day Q_s across all individuals per species showed that maple transported more water than oak through most of the season (Fig. 3a). Water transport in both species was initially low in the early summer due to a cool rainy period, but increased during typical hot and dry conditions of mid-July. During this period of maximum water use, maple moved approximately 2.5 times the water as oak. As is common in the region, there were few precipitation events during mid-summer (Fig. 3a, bars). Corresponding to this dry period, maple water use showed a gradual decline from its July maximum to values close to oak by summer's end. The decline in maple water use was associated with a decline in predawn xylem pressure (Fig. 3b, regression line; mid-day pressures were seasonably stable). Though generally lower than maple, oak water use was remarkably stable throughout the summer, as were predawn and mid-day xylem pressures (Fig. 3a, b). Late in the season, after the first frost (maximum and minimum temperatures shown in bold and gray, respectively, in Fig. 3a) sapflow in both species dropped sharply with little sapflow thereafter.

Maple whole-tree hydraulic conductance (K_s , standardized for tree size) averaged 1.7 times greater than oak with no seasonal trend (Fig. 3c). An outlier in maple (day 184; K_s of 3.6 standard deviations above the mean, datum not

Fig. 3 **a** Daily sapflow (Q_s , standardized for tree size) averaged across all trees per species versus day of year for *Acer grandidentatum* (maple, solid circles) and *Quercus gambelii* (oak, open circles). Maximum (black line) and minimum (gray line) daily temperatures and total daily precipitation (gray bars). Peak growing season delimited by vertical dotted lines (day 172–272). **b** Mean daily predawn (squares) and mid-day (triangles) xylem pressure for maple (solid symbols) and oak (open symbols). The only significant seasonal trend was a decrease in Maple predawn pressure (regression line). **c** Standardized whole-tree conductance (K_s) versus day of the year for maple (solid circles) and oak (open circles)



shown in Fig. 3c) was excluded. It was associated with a 10-mm rain event the day before and low VPD values during the middle of the measurement day which may have prevented near-steady state conditions required for accurate hydraulic conductance estimation. The generally greater rate of water use in maple was a result of its greater

K_s rather than greater ΔP because the mid-day ΔP at maximized transpiration did not statistically differ with tree size or between species ($\Delta P = 1.29 \pm 0.03$ MPa in maple, 1.32 ± 0.04 MPa in oak; von Allmen et al. 2012). The lack of a significant decrease in whole-tree conductance through the season suggests that the late-season decline in maple

sapflow (Fig. 3a) was due to dropping soil-to-leaf pressures ($\Delta P'$) rather than a decrease in hydraulic conductance from xylem cavitation ($Q_s = K_s \times \Delta P'$).

Partitioning tree hydraulic resistance into root–stem–leaf components

Tree hydraulic resistance in maple was fairly evenly distributed above and below ground with $57 \pm 7\%$ of tree hydraulic resistance (R_{tree}) residing in the shoot. Oak, in contrast, had a much greater portion of above-ground resistance, with $84 \pm 3\%$ of R_{tree} estimated in shoots (Fig. 4, pie charts). Thus, even though R_{tree} was less in maple than in oak, maple root resistance (R_{root}) was estimated to be greater than oak by a factor of 1.6–1.67 across the trunk diameter range studied (Fig. 4, R_{root} shown as “R” shaded portion in graphs).

The shoot resistances were partitioned into leaf (R_{leaf}) and stem (R_{stem}) components based on area-specific resistance of leaves (r_{leaf}) and leaf area per basal area (A_L/A_B). Maple r_{leaf} averaged $21.3 \pm 0.11 \text{ kPa s m}^2 \text{ mg}^{-1}$ (mean \pm SE, $n = 12$), and oak r_{leaf} averaged $16.5 \pm 3.53 \text{ kPa s m}^2 \text{ mg}^{-1}$ ($n = 11$). Neither species showed any relation between r_{leaf} and tree trunk diameter (D). When the area-specific r_{leaf} was scaled to total tree leaf resistance in parallel, R_{leaf} (using A_L/A_B estimates cited above), leaves exhibited similar collective resistances between species, with maple R_{leaf} being about 1.4 times less than oak (Fig. 4, R_{leaf} shown as “L” shaded portion in graphs).

The R_{leaf} as a percentage of R_{tree} was similar between species and ranged from an estimated 42–36% (maple-oak) in small trees (trunk $D = 5 \text{ cm}$) to 19–17% (maple-oak) in large trees ($D = 30 \text{ cm}$; Fig. 4 pie charts). The decline resulted from the assumption that leaf area increases with D^2 , and the observation that tree

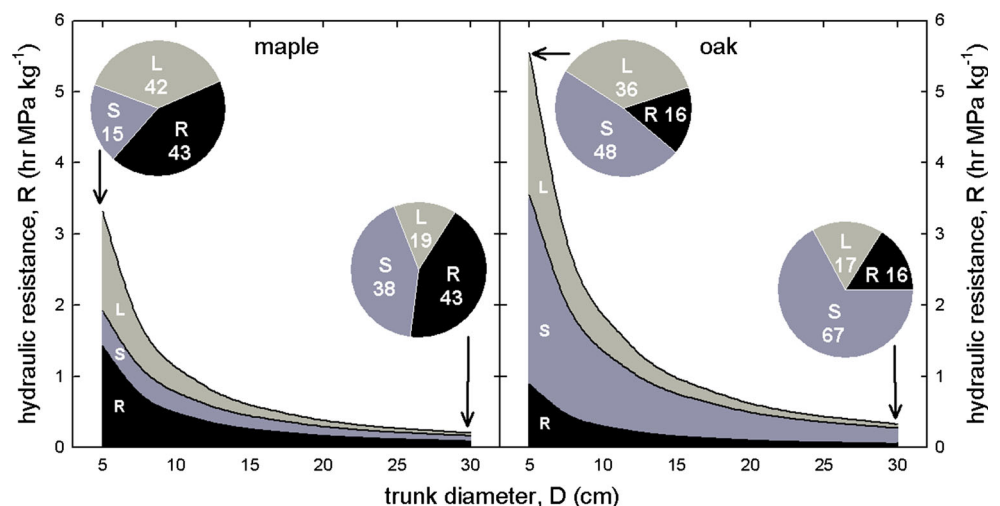
hydraulic conductance increased more slowly with $D^{q < 2}$ (Fig. 1). Hence, R_{leaf} decreased faster with trunk diameter than did R_{tree} . The decline in $\%R_{\text{leaf}}$ with tree size was necessarily mirrored by an increase in $\%R_{\text{stem}}$ (Fig. 4, pie charts) because the root resistance fraction was size invariant.

The main difference between the two species was the estimated stem resistance. The R_{stem} in maple was 5.4 ($D = 5 \text{ cm}$) to 2.8 ($D = 30 \text{ cm}$) times less than oak (Fig. 4, R_{stem} shown as shaded “S” portion of graphs). The R_{stem} as a percentage of R_{tree} rose from 15 to 38% (maple-oak) in small trees ($D = 5 \text{ cm}$) to 48–67% (maple-oak) in large ones ($D = 30 \text{ cm}$, Fig. 4, pie charts).

Biomass growth and cumulative water use

From previously reported tree height by trunk diameter scaling and wood densities for the study trees (von Allmen et al. 2012), we estimated that both species had similar shoot biomass growth rates (B) across all their years of growth (Fig. 5). Although maples were estimated to produce more leaf area per basal area, this was offset somewhat by their higher specific leaf area ($127 \pm 8 \text{ cm}^2 \text{ g}^{-1}$) vs. oak leaves ($100 \pm 8 \text{ cm}^2 \text{ g}^{-1}$). Focusing on the data for the 2009 year of our sap flux study, there were no significant differences in annual B by D scaling exponents and intercepts (Fig. 5, insert). Maple, however, showed more inter-annual variation in growth (Fig. 5, $r^2 = 0.73$) than oak ($r^2 = 0.89$). During 2009, maple growth rate scaled with trunk diameter to the 1.74 (1.49–1.99; RMA) power and the oak B by D exponent was 1.82 (1.52–2.11). The similarity between B by D scaling in Fig. 5 and Q_{max} by D scaling in Fig. 1 suggests a near-isometric relationship between water use and shoot biomass growth.

Fig. 4 Partitioning of tree hydraulic resistance into root (R), stem (S), and leaf (L) components. Resistances were calculated as continuous functions of trunk diameter (D), with the contributions of the three differently shaded components shown (component resistances sum to total tree value). Pie charts show percentages of whole-tree resistance in the three components for $D = 5 \text{ cm}$ and $D = 30 \text{ cm}$ trees



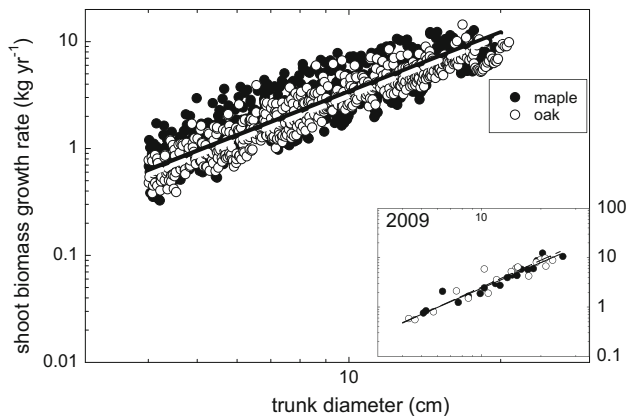


Fig. 5 Shoot biomass growth rate (above-ground stem + leaves) estimated from all growth rings of each sap flux tree vs. trunk diameter in *Acer grandidentatum* (maple, solid circles) and *Quercus gambelii* (oak, open circles). The linear regressions (RMA) are shown for maple (black solid line, $r^2 = 0.73$) and oak (white dashed line, $r^2 = 0.89$). Insert to right shows 2009 shoot biomass growth rates versus tree diameter; the similar RMA regressions are overlapping

To directly compare water use and growth during 2009, we added up the cumulative water used by each study tree over the 100 day peak growing season from late June through September (dotted vertical lines on Fig. 3a). For example, the largest maple ($D = 31$ cm) moved 5,690 kg of water and the largest oak ($D = 26$ cm) moved 2,307 kg. Maple biomass growth in 2009 scaled with its cumulative water use to the 0.95 (0.76–1.15; RMA) power compared to 1.08 (0.67–1.49) in oak (Fig. 6). Neither 95 % confidence limit excluded isometry, further supporting that growth was proportional to water use in each species. The exclusion of the low sap flow datum in oak did not alter this conclusion.

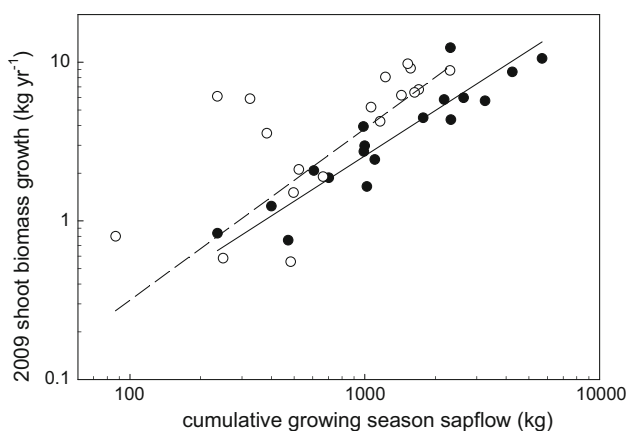


Fig. 6 Shoot biomass growth rate for 2009 for each individual tree versus cumulative whole-tree sapflow across the peak growing season (100 days between dotted lines in Fig. 3a) in *Acer grandidentatum* (maple, solid circles, solid RMA line, $r^2 = 0.85$) and *Quercus gambelii* (oak, open circles, dashed RMA line, $r^2 = 0.48$)

Although water consumption in both species was approximately proportional to shoot growth, the ratio of water use per growth was significantly different, implying a different coefficient of proportionality. Maple exhibited the greater growing season water consumption per annual shoot biomass growth. The mean ratio of cumulative water use over the 100 day peak growing season per annual 2009 biomass growth was 410 ± 30 kg water/kg shoot dry mass (mean \pm SE) in maple versus 250 ± 44 kg water/kg stem biomass in oak (means different at $p = 0.004$; independent samples t test). Thus, oak was an estimated 1.6 times more efficient at converting water use over the measurement period into annual shoot biomass than maple.

Discussion

The co-dominance of *Acer grandidentatum* (“maple”) and *Q. gambelii* (“oak”) was associated with similar shoot growth rates, but clear differences in water use strategy. For a given tree size, maple consumed more water by having greater tree hydraulic conductance and rising transpiration with VPD. However, maple uptake declined during the summer drought suggesting greater reliance on shallow soil water. Although study trees were within a riparian corridor, they were rooted far enough above the stream surface that shallow roots could experience soil water stress. Oak consumed less water due to lower tree hydraulic conductance and flat transpiration with VPD. But oak’s uptake was seasonably stable, suggesting a deeper water source. Despite using less water (roughly 40 % less than maple over the 100-day time frame in Fig. 3a), oak was able to approximate the shoot growth rate of maple (possibly an important factor for coexistence) by being much more efficient at exchanging water for shoot growth.

The contrasting water use was associated with the difference in stem anatomies between the two species. The difference in tree hydraulic conductance between the species was estimated to be largely localized to the stem (as opposed to leaves or roots), which is where the diffuse- vs. ring-porous anatomies are manifested (Gasson 1985; Jaquish and Ewers 2001). The maple stem network was estimated to have 2.8–5.4 times the hydraulic conductance of the oak stem system at mid-day (Fig. 4, shown as resistances). Previous measurements of native conductivity of excised stem segments from the same study site are in accord, with maple conductivity per stem area averaging approximately 2.5 times that of oak (Taneda and Sperry 2008).

The large diameter of the early wood vessels in ring-porous oak stems apparently failed to compensate for the greatly reduced number of vessels in the single functioning growth ring. The number of conducting vessels would be

reduced even further by cavitation and high native embolism as measured previously in the same watershed (Taneda and Sperry 2008; Christman et al. 2012). Although maple has narrower vessel diameters, there are many more vessels per wood area, and the total area of sapwood is much greater owing to multi-year functional life span (von Allmen et al. 2012). Furthermore, *A. grandidentatum* suffers little embolism at the study site owing to its high resistance to cavitation (Taneda and Sperry 2008). Neither species showed any decline in whole-tree hydraulic conductance (size normalized) over the growing season, suggesting that there was no significant accumulation of drought-induced cavitation. In maple, this is consistent with its cavitation resistance; in oak it is consistent with the lack of any seasonal drop in mid-day xylem pressure (Fig. 3b).

Perhaps because of maple's higher tree hydraulic conductance, maple trees supported more estimated leaf area than oak for the same trunk diameter (see also Taneda and Sperry 2008). Consequently, the two species exhibited similar rates of water use and hydraulic conductance per leaf area. Convergence of leaf area water use rates has been observed among other species (Mencuccini 2003; Zeppel 2013), and may result from the combination of a narrow range of optimal stomatal conductances and canopy xylem pressures (Mencuccini 2002; Holtta et al. 2011). For example, if oak increased its leaf area to match maple, oak would have to reduce significantly either its canopy xylem pressure, or its stomatal conductance. Although convergence in conductances and water use per leaf area may be important for the regulation of optimal gas exchange and pressure drop, divergence in water use at the whole-tree (size-standardized) level is relevant for understanding drivers of plant productivity, water use efficiency, and ecohydrology.

The comparison of whole-tree water use requires standardization for the typically large effect of tree size (Meinzer et al. 2001). Standardizing by sapwood area fails to standardize for tree size because trees of the same basal diameter and height, and hence "footprint" of occupied forest, can have vastly different sapwood areas (Zeppel 2013). For example, our *Q. gambelii* trees had many times greater water transport per sapwood area than *A. grandidentata* (data not shown), yet the oak trees consumed significantly less water for their basal diameter and overall size. However, even standardizing by total basal area only eliminates the size effect if the rate of water use scales 1:1 with basal area ($Q \propto D^q = 2$). Such was not the case in *A. grandidentatum* and *Q. gambelii*, where water use failed to keep pace with basal area, and $Q \propto D^{q < 2}$. Estimates from the literature suggest $1.5 < q < 2$ (Enquist et al. 2000; Meinzer et al. 2001, 2005; Mencuccini 2003; Sperry et al. 2012b; von Allmen et al. 2012), so this is apparently a

general conclusion. Water use expressed per basal area will, therefore, tend to decline with tree size, and fail as a standardization method across broad size ranges. Our expression of Q per D^q ensured a size-independent basis for whole-tree comparisons of water use and hydraulic conductance, as long as q was similar between species (as in our study). Conceptually, it is similar to comparing of Q by D scaling intercepts (log–log regression intercept = predicted Q/D^q). The approach may be generally useful if the empirical q range proves to be more limited than the theoretically possible range (Sperry et al. 2012b).

Our estimate for the partitioning flow resistances between stem and leaves assumed that unlike Q and K , the canopy leaf area does scale 1:1 with basal area within a species. This is a common assumption (Enquist and Niklas 2001; Niklas and Spatz 2004), but the data indicate considerable variation (Fownes and Harrington 1992; Bartelink 1997; Bond-Lamberty et al. 2002; Calvo-Alvarado et al. 2008). Nevertheless, it seems likely that leaf area increases faster with tree basal diameter than does Q and K , because Q and K expressed per leaf area tends to decline with tree size (Mencuccini and Grace 1996; Mencuccini 2003). A corollary is that the fraction of whole-tree flow resistance that resides in the leaves will also decrease with size (as long as the leaf-area-specific resistance is invariant with tree size) as estimated in Fig. 4. Our estimate that maple and oak leaves contribute at least 20–50 % to the total plant resistance is consistent with direct measurements in a variety of other species (Sack and Tyree 2005). Notably, our results indicate that roots, stems or leaves can be the pre-eminent source of whole-tree flow resistance depending on species and size (Fig. 4).

Shoot biomass growth showed a roughly proportional correspondence with growing season water use in both species. Oak, however, appeared to compensate for its lower water use with a 1.6-fold greater efficiency in converting water use to shoot biomass growth (Fig. 6). This efficiency is probably even greater given that *Q. gambelii* breaks bud almost a month later than maple at the study site (J.S. Sperry, pers obs) and has a consequently shorter total growing season. Other comparisons have noted more stable and ultimately greater allocation of carbon to growth with lifespan in ring- vs. diffuse-porous species, a trait that could enhance ring-porous water use efficiency (Genet et al. 2009). Other contributing factors could be lower long-term allocation to reproduction and greater fractional allocation to stems vs. roots in *Q. gambelii* vs. *A. grandidentatum*. *Q. gambelii* is a highly clonal species via root sprouts from lignotubers (Tiedemann et al. 1987), and most oaks at the study site, even the smaller trees, are likely connected to large clonal root systems (reproduction by seed is rare in the study region; Neilson and Wullstein 1983). Access to a large root system is consistent with

oak's lower root system resistance (Fig. 4) compared to maple. The extensive clonal root system may require less annual growth and maintenance once it is established.

Our inference of deeper roots in *Q. gambelii* vs. *A. grandidentatum* is consistent with other studies from the region (Tiedemann et al. 1987; Philips and Ehleringer 1995; Taneda and Sperry 2008). Deeper roots coupled with a strong VPD response was consistent with seasonally very stable rates of water use in oak vs. the more environmentally responsive variation in maple. The projection of consistent inter-annual rates of water use by oak is mirrored by its relatively invariant annual growth rates (Fig. 5, $r^2 = 0.89$). In contrast, maple showed more variation in growth rate between years (Fig. 5, $r^2 = 0.73$), consistent with what we suspect would be greater inter-annual variation in water use. The contrast of long-term stability of growth in *Quercus* vs. variable growth in diffuse-porous co-dominants has also been observed in other comparative studies (Genet et al. 2009).

This comparative study of two co-dominant species exposes both generalities and particularities in their hydraulics and growth. Both species converge on similar size-scaling of water use, leaf-area-based hydraulic conductance, xylem pressure drop, shoot growth rates, and proportional exchange of water for shoot biomass. The species diverge by being good at different things. Maple is better at moving water when it is available, and oak is more efficient at converting a unit of water into shoot growth.

It is possible that these contrasting traits may apply to ring- and diffuse-porous species generally. Water use per basal area has been observed to be substantially less in ring-porous vs. co-occurring diffuse-porous trees in the eastern deciduous forest of the USA (Pataki and Oren 2003; Bovard et al. 2004). Ring-porous *Quercus* species of that region were also less responsive to soil moisture in the top 50 cm, suggesting deeper root systems vs. diffuse-porous trees (Meinzer et al. 2013) as inferred in from our comparison. There is also evidence for greater and more stable lifetime allocation to shoot growth in ring-porous species, suggesting higher water use efficiency and less response to environmental variation than in diffuse-porous species (Genet et al. 2009). Caveats complicate the comparison, however, because whole-tree water use is often not appropriately size-standardized, and standard Granier coefficients are not necessarily applicable in ring-porous species (Bush et al. 2008; Taneda and Sperry 2008; Bush et al. 2010; von Allmen et al. 2012). Some studies support the coordination of vulnerability to cavitation and a flat transpiration vs. VPD pattern in ring-porous trees, suggestive of a maximally sensitive stomatal response to VPD (Bush et al. 2008; Litvak et al. 2012). However, ring-porous *Quercus* of the eastern deciduous forest were found to increase transpiration with VPD to a greater extent than co-

occurring diffuse-porous species (Meinzer et al. 2013). Furthermore, there is some controversy about how accurately cavitation vulnerability can be measured in large-vessel species (Cochard et al. 2010; Sperry et al. 2012a). It is not clear by what mechanism(s) vessel size is linked to water stress-induced cavitation (Lens et al. 2010), and some ring-porous trees may have evolved ways of achieving large and long vessels without increasing vulnerability. While the coexistence of ring- and diffuse-porous trees in many temperate forests demonstrates compatibility, whether their functional differences are consistent in every case awaits further study.

Author contribution statement EIV and JSS conceived and designed the experiments; EIV conducted the experiments with assistance from SEB; EIV and JSS analyzed the data and wrote the manuscript; SEB commented on manuscript drafts.

Acknowledgments We thank Henry Grover and Andy Crowl for field assistance, and Kevin Hultine for technical support of sapflow measurements and calibrations, and Duncan Smith and Mairgereth Christman for technical help in the laboratory. Fred Adler (University of Utah) assisted with data analysis and interpretation. The authors were supported from National Science Foundation grant ATB-0742800; JSS and EIV received additional funding from National Science Foundation grant-IBN-0743148.

Conflict of interest The authors declare that they have no conflict of interest.

References

- Alder NN, Sperry JS, Pockman WT (1996) Root and stem xylem embolism, stomatal conductance, and leaf turgor in *Acer grandidentatum* populations along a soil moisture gradient. *Oecologia* 105:293–301
- Barbour MG, Billings WD (eds) (1988) North American terrestrial vegetation. Cambridge University Press, New York
- Bartelink HH (1997) Allometric relationships for biomass and leaf area of beech (*Fagus sylvatica* L.). *Ann Sci For* 54:39–50
- Bond-Lamberty B, Wang C, Gower ST (2002) Aboveground and belowground biomass and sapwood area allometric equations for six boreal tree species of northern Manitoba. *Can J For Res* 32:1441–1450
- Bovard BD, Curtis PS, Vogel CS, Su HB, Schmid HP (2004) Environmental controls on sapflux in a northern hardwood forest. *Tree Physiol* 25:31–38
- Bush SE, Pataki DE, Hultine KR, West AG, Sperry JS, Ehleringer JR (2008) Wood anatomy constrains stomatal responses to atmospheric vapor pressure deficit in irrigated, urban trees. *Oecologia* 156:13–20
- Bush SE, Hultine KR, Sperry JS, Ehleringer JR (2010) Calibration of thermal dissipation sap flow probes for ring- and diffuse-porous trees. *Tree Physiol* 30:1545–1554
- Calvo-Alvarado JC, McDowell NG, Waring RH (2008) Allometric relationships predicting foliar biomass and leaf area: sapwood area ratio from tree height in five Costa Rican rain forest species. *Tree Physiol* 28:1601–1608

- Christman MA, Sperry JS, Smith DD (2012) Rare pits, large vessels, and extreme vulnerability to cavitation in a ring-porous tree species. *New Phytol* 193:713–720
- Cochard H, Herbette S, Barigah T, Vilagrosa A (2010) Does sample length influence the shape of vulnerability to cavitation curves? A test with the Cavitron spinning technique. *Plant, Cell Environ* 33:1543–1552
- Davis SD, Sperry JS, Hacke UG (1999) The relationship between xylem conduit diameter and cavitation caused by freeze-thaw events. *Am J Bot* 86:1367–1372
- Ehleringer JR, Arnow LA, Arnow T, McNulty IB, Negus NC (1992) Red Butte Canyon Research Natural Area: history, flora, geology, climate, and ecology. *Great Basin Natural* 52:95–121
- Enquist BJ, Niklas KJ (2001) Invariant scaling relations across tree-dominated communities. *Nature* 410:655–660
- Enquist BJ, West GB, Brown JH (2000) Quarter-power allometric scaling in vascular plants: Functional basis and ecological consequences. In: Brown JH, West GB (eds) *Scaling in Biology*. Oxford University Press, Oxford, pp 167–198
- Fownes JH, Harrington RA (1992) Allometry of woody biomass and leaf area in five tropical multipurpose trees. *J Trop For Sci* 4:317–330
- Gasson P (1985) Automatic measurement of vessel lumen area and diameter with particular reference to pedunculate oak and common beech. *IAWA Bull* 6:219–237
- Genet H, Breda N, Dufrene E (2009) Age-related variation in carbon allocation at tree and stand scation during winter and recovery of hydraulic conductivity in diffuse-porous and ring-porous trees. *Oecologia* 105:435–439
- Granier A (1985) Une nouvelle methode pour la mesure du flux de seve brute le tronc des arbres. *Ann Sci For* 42:193–200
- Hacke U, Sauter JJ (1996) Xylem dysfunction during winter and recovery of hydraulic conductivity in diffuse-porous and ring-porous trees. *Oecologia* 105:435–439
- Hacke UG, Sperry JS, Wheeler JK, Castro L (2006) Scaling of angiosperm xylem structure with safety and efficiency. *Tree Physiol* 26:689–701
- Holtta T, Mencuccini M, Nikinmaa E (2011) A carbon cost-gain model explains the observed patterns of xylem safety and efficiency. *Plant Cell Environ* 34:1819–1834
- Jaquish LL, Ewers FW (2001) Seasonal conductivity and embolism in the roots and stems of two clonal ring-porous trees, *Sassafras albidum* (Lauraceae) and *Rhus typhina* (Anacardiaceae). *Am J Bot* 88:206–212
- Lens F, Sperry JS, Christman MA, Choat B, Rabaey D, Jansen S (2010) Testing hypotheses that link wood anatomy to cavitation resistance and hydraulic conductivity in the genus *Acer*. *New Phytol* 190:709–723
- Litvak E, McCarthy HR, Pataki DE (2012) Transpiration sensitivity of urban trees in a semi-arid climate is constrained by xylem vulnerability to cavitation. *Tree Physiol* 32:373–388
- Meinzer FC, Goldstein G, Andrade JL (2001) Regulation of water flux through tropical forest canopy trees: do universal rules apply? *Tree Physiol* 21:19–26
- Meinzer FC, Bond BJ, Warren JM, Woodruff DR (2005) Does water transport scale universally with tree size? *Funct Ecol* 19:558–565
- Meinzer FC, Woodruff DR, Eissenstad DM, Lin HS, Adams TS, McCulloh KA (2013) Above- and belowground controls on water use by trees of different wood types in an eastern US deciduous forest. *Tree Physiol* 33:345–356
- Mencuccini M (2002) Hydraulic constraints in the functional scaling of trees. *Tree Physiol* 22:553–565
- Mencuccini M (2003) The ecological significance of long-distance water transport: short-term regulation, long-term acclimation and the hydraulic costs of stature across plant life forms. *Plant Cell Environ* 26:163–182
- Mencuccini M, Grace J (1996) Developmental patterns of above-ground hydraulic conductance in a Scots pine (*Pinus sylvestris* L.) age sequence. *Plant Cell Environ* 19:939–948
- Neilson RP, Wullstein LH (1983) Biogeography of two southwest American oaks in relation to atmospheric dynamics. *J Biogeogr* 10:275–297
- Niklas KJ, Spatz HC (2004) Growth and hydraulic (not mechanical) constraints govern the scaling of tree height and mass. *Proc Natl Acad Sci USA* 101:15661–15663
- Pataki DE, Oren R (2003) Species differences in stomatal control of water loss at the canopy scale in a mature bottomland deciduous forest. *Adv Water Resour* 26:1267–1278
- Philips SL, Ehleringer JR (1995) Limited uptake of summer precipitation by bigtooth maple (*Acer grandidentatum* Nutt.) and Gambel's oak (*Quercus gambelii* Nutt.). *Trees* 9:214–219
- Sack L, Tyree MT (2005) Leaf hydraulics and its implications in plant structure and function. In: Holbrook NM, Zwieniecki MA (eds) *Vascular Transport in Plants*. Elsevier/Academic Press, Oxford, pp 93–114
- Sack L, Melcher PJ, Zwieniecki MA, Holbrook NM (2002) The hydraulic conductance of the angiosperm leaf lamina: a comparison of three measurement methods. *J Exp Bot* 53:2177–2184
- Sperry JS, Donnelly JR, Tyree MT (1988) Seasonal occurrence of xylem embolism in sugar maple (*Acer saccharum*). *Am J Bot* 75:1212–1218
- Sperry JS, Christman MA, Smith DD (2012a) Vulnerability curves by centrifugation: is there an open vessel artifact, and are “r” shaped curves necessarily invalid? *Plant Cell Environ* 35:601–610
- Sperry JS, Smith DD, Savage VM, Enquist BJ, McCulloh KA, Reich PB, Bentley LP, Von Allmen EI (2012b) A species-level model for metabolic scaling in trees I. Exploring boundaries to scaling space within and across species. *Funct Ecol* 26:1054–1065
- Taneda H, Sperry JS (2008) A case-study of water transport in co-occurring ring- versus diffuse-porous trees: contrasts in water-status, conducting capacity, cavitation and vessel refilling. *Tree Physiol* 28:1641–1652
- Tiedemann AR, Clary WP, Barbour RJ (1987) Underground systems of Gambel Oak (*Quercus gambelii*) in central Utah. *Am J Bot* 74:1065–1071
- von Allmen EI, Sperry JS, Smith DD, Savage VM, Enquist BJ, Reich PB, Bentley LP (2012) A species level model for metabolic scaling of trees II. Testing in a ring- and diffuse-porous species. *Funct Ecol* 26:1066–1076
- Wang J, Ives NE, Lechowicz MJ (1992) The relation of foliar phenology to xylem embolism in trees. *Funct Ecol* 6:469–475
- Warton DI, Wright IJ, Falster DS, Westoby M (2006) Bivariate line-fitting methods for allometry. *Biol Rev* 81:259–291
- Zeppel M (2013) Convergence of tree water use and hydraulic architecture in water-limited regions: a review and synthesis. *Ecohydrology*. doi:10.1002/eco.1377
- Zimmermann MH (1983) *Xylem structure and the ascent of sap*. Springer, Berlin, Heidelberg, New York